A close coupling study of the bending relaxation of H 2 O by collision with He

Thierry Stoecklin, Lisán David Cabrera-González, Otoniel Denis-Alpizar, Dayán Páez-Hernández

A Close Coupling study of the Bending relaxation of H_2O by collision with He

Thierry Stoecklin,[1, a)] Lisán David Cabrera-González,[2] Otoniel Denis-Alpizar,[3, b)] and Dayán Páez-Hernández[2]
[1)] *Institut des Sciences Moléculaires, Université de Bordeaux, CNRS UMR 5255, 33405 Talence Cedex, France*
[2)] *Doctorado en Fisicoquímica Molecular, Facultad de Ciencias Exactas, Universidad Andres Bello, República 275, Santiago, Chile*
[3)] *Núcleo de Astroquímica y Astrofísica, Instituto de Ciencias Químicas Aplicadas, Facultad de Ingeniería, Universidad Autónoma de Chile, Av. Pedro de Valdivia 425, Providencia, Santiago, Chile*

(Dated: 25 March 2021)

We present a close-coupling study of the bending relaxation of H_2O by collision with He, taking explicitly into account the bending-rotation coupling within the Rigid-Bender close-coupling (RB-CC) method. A 4D potential energy surface is developed based on a large grid of *ab initio* points calculated at the CCSD(T) level of theory. The bound states energies of the He-H_2O complex are computed and found to be in excellent agreement with previous theoretical calculations. The dynamics results also compare very well with the rigid rotor results available in the Basecol database and with experimental data for both rotational transitions and bending relaxation. The bending rotation coupling is also demonstrated to be very efficient in increasing bending relaxation when the rotational excitation of H_2O increases.

I. INTRODUCTION

The vibrational relaxation of H_2O molecules is involved in many chemical and physical processes. The detailed knowledge of the vibrational relaxation rates in the gas phase is, for example, needed to model atmospheric processes, for understanding high-temperature dynamics of combustion product gases, of which H_2O is a major component or for optimizing H_2O lasing processes. It is also one of the most common molecules in the interstellar medium (ISM) where it has been observed in a wide variety of astronomical environments ranging from molecular clouds to stellar photospheres, circumstellar envelopes, and comets[1]. In the ISM or the earth mesosphere and thermosphere, the density and temperatures are very often such as there is no local thermodynamic equilibrium and spontaneous emission processes compete with collisional relaxation processes. While the Einstein coefficients are usually known, the collisional rate coefficients with the most common colliders (e.g.,H,H_2,He) need to be determined in order to analyse the physical-chemical conditions.

Several sets of calculated rate coefficients have been reported in the last decades for the collision of H_2O with He[2–5] and H_2[6–9]. However, these rate coefficients concern mostly pure rotational transitions. Among the only two theoretical studies including the H_2O vibration, the one of Faure *et al.*[10,11] used the quasi-classical trajectory (QCT) method while the only quantum study was performed by some of us[12] for the collisions of H_2O with H_2 using our recently developed Rigid-Bender Close-Coupling (RB-CC) method which includes explicitly the bending-rotation coupling for a triatomic molecules colliding with an atom. This work extended our previous studies dedicated to the collisions of linear triatomic molecules with atoms when including explicitly the bending-rotation coupling as for HCN[13,14], DCN[15] and C_3[16–18] colliding with He.

The coupling between rotation and vibration was also considered by Dagdigian and Alexander[19] when treating the umbrella mode of CH_3 colliding with He and by Loreau and Van der Avoird considering the umbrella mode of NH_3 colliding with He[20]. However, a direct comparison with experiment was not possible for any of theses systems in the absence of experimental data.
In another work, Ma, Dagdigian and Alexander also considered the bending relaxation of CH_2 by collision with helium.[21,22]. They calculated a 4D PES for this system including the bending motion and averaged it over rigid bender CH_2 functions. They obtained the first quantum estimate of the bending relaxation rate coefficient for this system. The coupling between bending and rotation was however only partially taken into account within this approach as the rotational dependence of the CH_2 rigid bender functions was neglected.
In the present work, we employ the RB-CC method to study the bending relaxation of H_2O by collisions with He for which experimental data are available.[23] In the work of Kung and Center[23] the vibrational relaxation of H_2O by several atoms and molecules was studied in a shock tube. In the case of H_2O + He, they only provided the value of the vibrational de-excitation rate coefficients (of the bending mode) at 2500 K, $k = 6.1 \times 10^{-12}$ cm^3**molecule**$^{-1}$ s^{-1} with a factor two uncertainty. The paper is organised as follows. In section 2 we present the calculations and the fitting of the four dimensional (4D) PES including the bending of H_2O and we remind the main steps of the RB-CC calculations. In section 3 the results are presented and discussed, while in the section 4. we present a few concluding remarks.

[a)] Electronic mail: thierry.stoecklin@u-bordeaux.fr
[b)] Electronic mail: otoniel.denis@uautonoma.cl

II. THEORY

A. PES calculations

Hou *et al.*[24] recently developed a PES for the H_2O + He system using the normal modes of H_2O, which they used for predicting the infra-red spectra of the complex. Here, a full PES describing also accurately the long-range dissociation of the He-H_2O complex is required to perform collisional dynamics calculations including the bending motio-n. We then devellopped a new 4D intermolecular PES $V(\gamma, R, \theta, \phi)$ which is presented below.

A large grid of *ab initio* energies was computed at the CCSD(T) level of theory using an aug-cc-pVQZ[25] basis set supplemented by a set of mid bond functions[26]. All calculations were performed with the MOLPRO package[27], and the basis Set superposition error was corrected with the counterpoise procedure[28].

The coordinate system for treating the collision of H_2O with He is shown in Fig. 1. The H_2O molecule lies in the XoZ plane, and the Z-axis is bisecting the bending angle γ. For each γ value the position of the center of mass is then slightly shifted. The origin of the coordinate system is the H_2O center of mass and the oxygen atom is on the positive side of the z axis. **The modulus of the intermolecular vector $\overrightarrow{R}$ connecting the H_2O center of mass to the helium atom is denoted R while θ is the angle between the z axis and the intermolecular vector $\overrightarrow{R}$,** and φ is the azimuthal angle. The OH distance was fixed at 0.957 Å[29].

15 428 *ab initio* energies were computed on a grid including seven values of the bending angles γ ranging from 70° to 140°, 29 values of R between 1.1 and 11 Å, 19 values of θ in the $(0, 180)$ interval, and 4 values of φ in steps of 30° in the $(0, 90)$ interval.

The short $V^{(SR)}(\gamma, R, \theta, \phi)$ and long-range $V^{(LR)}(\gamma, R, \theta, \phi)$ parts of the PES were fitted independently and then assembled using a switching function S(R). The global intermolecular potential thus takes the following analytical form .

$$V(\gamma, R, \theta, \phi) = S(R)V^{(SR)}(\gamma, R, \theta, \phi) + (1 - S(R))\, V^{(LR)}(\gamma, R, \theta, \phi) \quad (1)$$

with

$$V^{(SR)}(\gamma, R, \theta, \phi) = \sum_{l=0}^{18} \sum_{m=0}^{min(l,6)} F_{lm}^{(SR)}(\gamma, R)\, \bar{P}_l^m(\cos\theta)\cos(m\varphi), \quad (2)$$

and

$$V^{(LR)}(\gamma, R, \theta, \phi) = \sum_{l=0}^{4} \sum_{m=0}^{l} F_{lm}^{(LR)}(\gamma, R)\, \bar{P}_l^m(\cos\theta)\cos(m\varphi), \quad (3)$$

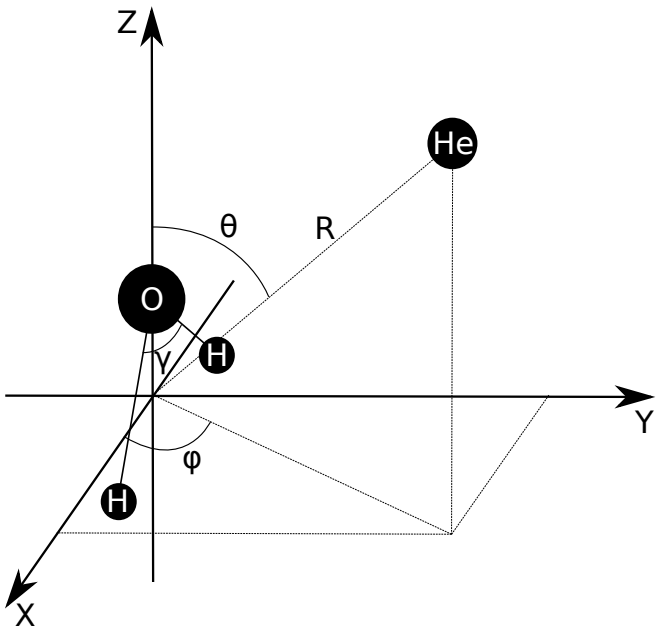

FIG. 1. Coordinates used for describing the interaction of H_2 O with He. The H_2O molecule lies in the XOZ plane and its center of mass is taken to be the origin of the frame.

while

$$S(R) = \frac{\mathrm{erfc}(A_0(R - R_0))}{2} \quad (4)$$

In these expressions only even values of m were used as a result of the C_{2v} symmetry of the H_2O molecule while $A_0 = 6$ Å^{-1}, and $R_0 = 4.5$Å.

For given values of R and γ, he F_{lm} coefficients were obtained by a least-square procedure. These coefficients where then fitted using the Reproducing Kernel Hilbert Space method of Ho and Rabitz[30],

$$F_{lm}^{(SR)or(LR)}(\gamma, R) = \sum_{i=1}^{N_R \cdot N_\gamma} \alpha_{lmi}^{(SR)or(LR)} q^{2,5}(R, R_i) q^2(z, z_i) \quad (5)$$

with $z(\gamma) = \frac{1-\cos\gamma}{2}$, and where the $q^{2,5}$ and q^2 are the

one dimensional kernels[30]

$$q^{2,5}(R,R_i) = \frac{2}{21R_>^6} - \frac{R_<}{14R_>^7}, \quad (6)$$

$$q^2(z,z_i) = 1 + z_< z_> + 2\left(z_<^2\right) z_> \left(1 - \frac{z_<}{3z_>}\right), \quad (7)$$

N_R and N_γ are the number of R and γ values of the *ab initio* grid. $R_<$ and $R_>$ are the lower and larger values of R and R_i, and $z_<$ and $z_>$ are the lower and larger values of z and z_i. The α_{lmi} coefficients were obtained by solving the linear equations system $\mathbf{Q}(x_k,x_{k'})\alpha_{lm}(x_{k'}) = \mathbf{F}_{lm}(x_k)$, where $\mathbf{Q}(x_k,x_{k'}) = q^{2,5}(R_k,R_{k'})q^2(z_k,z_{k'})$,

B. Dynamics

We use the rigid bender Close Coupling (RB-CC) method which was already presented in details in previous papers[31]. Also, only the main steps of the method are only briefly reminded.

1. Rigid bender description of H_2O

The symmetric form of the rigid-bender restriction of the Hamiltonian $H^{RB}(H_2O)$ developed long ago by Carter *et al.*[32] for centrosymmetric triatomics is used to model the coupled bending and rotation degrees of freedom of H_2O. This hamiltonian is diagonalised in the symmetrised rovibrational basis set $|jn\bar{K}m_j,p\rangle$ suggested by Tennyson[33] :

$$|jn\bar{K}m_j,p\rangle = \frac{1}{\sqrt{2(1+\delta_{\bar{K}0})}}[|jn\bar{K}m_j\rangle + (-1)^p|jn-\bar{K}m_j\rangle] \quad (8)$$

with

$$|jn\bar{K}m_j\rangle = P_n^{\bar{K}}(\cos\gamma)|j\bar{K}m_j\rangle \quad (9)$$

where, the ket $|jKm_j\rangle$ is a symmetric top wavefunction while m_j and K are the projections of the rotational angular momentum j of H_2O along the space fixed z-axis and along the molecular fixed z-axis respectively. $P_n^{\bar{K}}(\cos\gamma)$ is a normalized associated Legendre polynomial describing the vibrational bending motion. The matrix elements of $H^{RB}(H_2O)$ in this basis set are given in many papers like[34] or more recently[35].

The diagonalisation of the triatomic Hamiltonian in this basis set gives the parity selected rigid-bender energies $\varepsilon^p_{\nu j\tau}$ and the eigenfunctions

$$\chi^{m_j p}_{\nu j\tau}(\gamma) = \sum_{n\geq\bar{K}}\sum_{\bar{K}\geq 0} C^{\nu j\tau p}_{n\bar{K}}|jn\bar{K}m_j,p\rangle = \sum_{\bar{K}\geq 0}\frac{\Gamma^{\nu j\tau p}_{\bar{K}}(\gamma)}{\sqrt{2(1+\delta_{\bar{K}0})}} \times \left[|j\bar{K}m_j\rangle + (-1)^{p+\bar{K}}|j-\bar{K}m_j\rangle\right] \quad (10)$$

where

$$\Gamma^{\nu j\tau p}_{\bar{K}}(\gamma) = \sum_{n\geq\bar{K}} C^{\nu j\tau p}_{n\bar{K}} P_n^{\bar{K}}(\cos\gamma) \quad (11)$$

ν is the bending quantum number of water and τ defines the rotational level of water inside a given j multiplet $-j \leq \tau \leq j$. In what follows we will also use instead of τ the alternative equivalent notation K_AK_C where $\tau = K_A - K_C$ and K_A and K_C are respectively the absolute values of the Z molecular axis projections of j respectively in the limit of a prolate or an oblate top.

2. Close Coupling equations

The rigid-bender wave-functions are then coupled with those describing the motion of the He projectile relative to H_2O in space fixed coordinates as:

$$|\nu j\tau p,l;JM\rangle = \sum_{m_j}\sum_{m_l}\sqrt{\tfrac{2J+1}{4\pi}}\langle jm_j lm_l|JM\rangle Y_l^{m_l}(\widehat{R}) \times \sum_{\bar{K}\geq 0}\frac{\tilde{\Gamma}^{\nu j\tau p}_{\bar{K}}(\gamma)}{\sqrt{2(1+\delta_{\bar{K}0})}}\left[|j\bar{K}m_j\rangle + (-1)^{p+\bar{K}}|j-\bar{K}m_j\rangle\right] \quad (12)$$

where $\widehat{R} \equiv (\theta_R,\varphi_R)$ designates the $\vec{R}$ polar and azimuthal angles in the space fixed frame while l and m_l are respectively the relative angular momentum quantum number and its projection along the z space fixed axis.

The expansion of the wave function of the system in this basis set gives the rigid-bender close-coupling equations for an atom colliding with a triatom bent at equilibrium.

$$\{[\frac{d^2}{dR^2} - \frac{l(l+1)}{R^2} + k^2_{\nu j\tau}]\delta_{\nu\nu'}\delta_{jj'}\delta_{\tau\tau'}\delta_{ll'} - [U]^{JM}_{\nu j\tau l;\nu' j'\tau' l'}\}(R) \times G^{JM}_{\nu j\tau l;\nu' j'\tau' l'}(R) = 0 \quad (13)$$

where $G^{JM}_{\nu j\tau l;\nu' j'\tau' l'}(R)$ is the radial part of the atom rigid bender scattering wave function, $k^2_{\nu j\tau} = 2\mu[E-\varepsilon_{\nu j\tau}]$ and

$$[U]^{JM}_{\nu j\tau l;\nu' j'\tau' l'}(R) = 2\mu\langle\nu j\tau lJM|V(\gamma,R,\theta,\phi)|\nu' j'\tau' l' JM\rangle = 2\mu\int_0^\pi d\gamma\sin(\gamma)\times \sum_{\bar{K},\bar{K}'}[\tilde{I}^{\nu j\tau p}_{\bar{K}}(\gamma) \times W^{JM}_{\nu jKlp;\nu' j'K'l'p'}(R) \times \tilde{I}^{\nu' j'\tau' p'}_{\bar{K}'}(\gamma)] \quad (14)$$

In the left hand side of this expression there is no mention of the quantum numbers p and p' as they are implicitly defined by the pseudo-quantum numbers τ and τ'. The $W^{JM}_{\nu jKlp;\nu' j'K'l'p'}(R)$ are the usual symmetrised combinations of the symmetric top matrix elements of the potential as given by Green[36].

III. RESULTS

A. PES

The agreement between the fitted and *ab initio* energies is quite satisfactory. The root means square deviation

TABLE I. Comparison between our results and those available in the literature for the equilibrium geometries and energies of the He-H_2O complex. (R is reported in Å, θ and φ in degree, and the energy in cm^{-1}).

PES	(R , θ, φ)	Energy
This work	(3.13, 76.43, 0)	-34.55
Ref.[24] (2016)	(3.14, 76.2, 0)	-34.09
Ref.[37] (2003)	(3.18, 79, 0)	-30.42
Ref.[38] (2002)	(3.13, 75, 0)	-34.90
Ref.[39] (2002)	(3.12, 78.3, 0)	-34.94

in cm^{-1} (RMSD) is equal to 1.73×10^{-2} for negative energies and to 2.04×10^{-3} for positive energies between 0 and 5000 cm^{-1}.

The global minimum of the PES, -34.55 cm^{-1} is obtained for the averaged[29] bending angle $\gamma = 104.42°$ and is associated with the bent configuration ($R = 3.13\mathring{A}$, $\theta = 76.43°$ and $\varphi = 0°$). This is in very good agreement with values reported in previous works as illustrated in Table III A.

Our four-dimensional PES shows a strong dependence in the bending angle γ in the region of the well, as illustrated in Fig. 2 where contour plots of the PES are represented for different value of γ and φ.[12,14,18].

B. Rigid-bender levels of H_2O

The details of these calculations can be found in our recent work.[31] When compared with experiment the average relative errors of the RB energies are respectively 2% and 3% in the fundamental and first excited bending levels of water. In order to focus on purely dynamical effects, we choose to fix the rovibrational energies of water at their experimental values[40] while keeping the expansion coefficients of these levels in a symmetrised symmetric top basis set to those obtained either by the rigid-bender or the rigid-rotor approach.

C. He-H_2O complex bound states calculations

In order to check the quality of our new PES we calculated the bound states of the He-H_2O complex and compare them with the most recent previous calculations available.[24] We performed calculations both at the Rigid Rotor level(denoted RR) for the equilibrium bending angle of free water as well as rigid bender calculations. For the latter calculations, we use the same variational approach described in some of our previous works. The wave function of the system is expanded in the coupled basis set defined in Eq. 12 describing the bending-rotation of H_2O and the relative movement of He towards H_2O. We then solve variationally equation Eq. 13 using a 200 points Chebyshev DVR grid along R spanning the [3,20] a_0 interval with 100 rotational basis functions included for each spin isomer of H_2O.

As can be seen in Table II the RR and RB results differ at the most by 0.02 cm^{-1} confirming the very good performance of the rigid rotor approximation for this system. We also obtain an excellent agreement with the calculations of Hou *et al.*[24] using our new PES. Our bound state energies are in average about 0.1 cm^{-1} lower than theirs as a result of the deeper well depth of our PES while the differences of energies between two different levels calculated by Hou *et al.*[24] are even in closer agreement with ours, demonstrating the good accuracy of our PES.

D. Dynamics

Our new surface was employed to perform both rigid asymmetric top (RAST-CC) and rigid bender (RB-CC) close coupling calculations using the Newmat code[31]. Ten values of the water rotational quantum number j were included in the H_2O rotational basis set while the RB-CC calculations involved two bending levels. Scattering calculations were carried out for energies up to 10000 cm^{-1} for each H_2O–He pair of nuclear spin modifications. The collision energy dependence of the computed vibrational quenching cross sections are fitted by power laws in the [500,10000] cm^{-1} interval. The resulting power law coefficients are then used to obtain the vibrational quenching rates above 500 K. This range of energies could involve exited bending and stretching levels of H_2O while the H_2O stretching modes are not taken into account in the present work. Error resulting from this approximation is, however expected to be very small while taking place only for the highest energies. Partial waves up to total angular momentum J = 125 were included in the calculations to achieve a 10^{-3} relative criterion for the convergence of the state-selected quenching cross section as a function of the maximal value of the total angular momentum quantum number J. The maximum propagation distance was 30 Bohr, and convergence was checked as a function of the propagator step size.

1. Rotational transitions inside the same bending level

We first performed RAST-CC calculations inside the fundamental bending state and compared them with those available in the Basecol[41] data base. The Basecol data was calculated by Yang *et al.*[42] using the Symmetry-adapted perturbation theory PES named (SAPT-P) of Patkowski *et al.*[38] . An example of comparison between our results and those of Yang *et al.*[42] is shown in Fig. 3 for transitions issued from the 3_{03} or 3_{13} levels. The relative average difference between our results and those of Yang *et al.* is equal to 30% as a result of both the differences between the two PES and the smaller rotational basis set used for the dynamics by

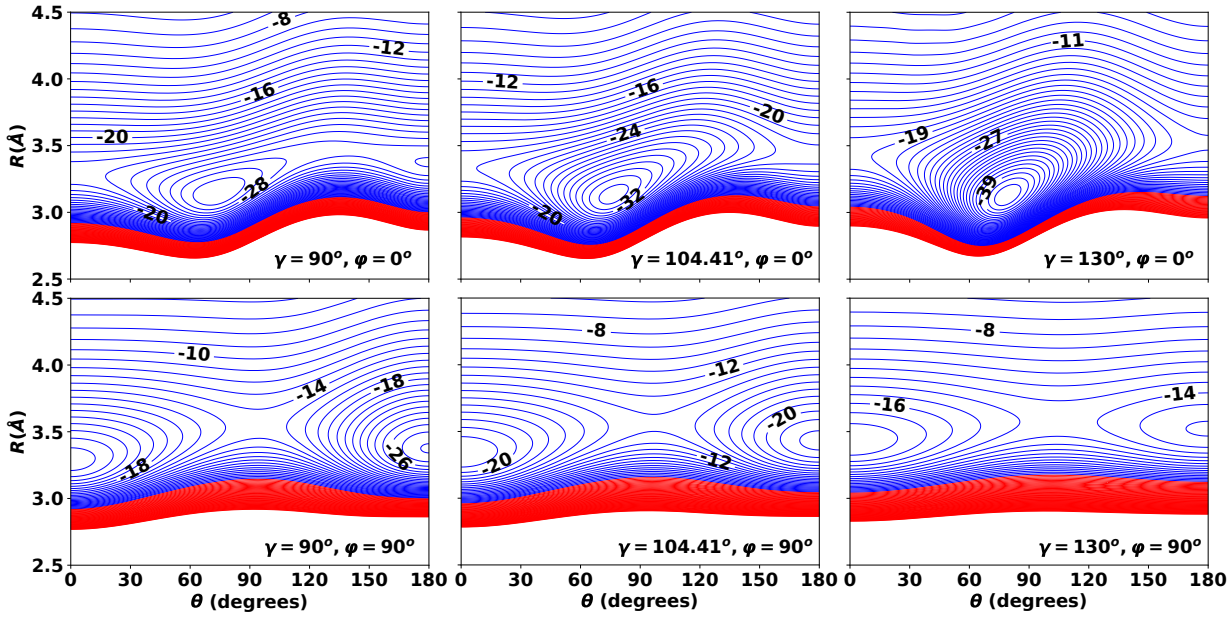

FIG. 2. Contour plot of the H_2O+He complex for several values of γ and φ. Negative (blue line) and positive energies (red lines) are both reported in steps of 1 cm^{-1}

TABLE II. Comparison between the bound states energies of the He-H_2O complex calculated with our PES at the Rigid Rotor (RR) and Rigid bender (RB) level with those (given between parenthesis) published by Hou *et al.*[24]

		J=0	J=1	J=2	J=3	J=4
He + *para*-$H_2O(\nu_2=0)$						
$\Sigma(0_{00})^e$	RR	-6.874	-6.196	-4.857	-2.901	-0.416
	RB	-6.870	-6.192	-4.854	-2.898	-0.413
		(-6.758)	(-6.083)	(-4.750)	(-2.801)	(-0.323)
$\Pi(1_{11})^e$	RR		30.052	30.723	32.010	33.784
	RB		30.043	30.713	32.002	33.784
			(30.370)	(31.030)	(32.330)	(34.216)
$\Pi(1_{11})^f$	RR		30.990	32.331	34.292	36.782
	RB		30.970	32.312	34.273	36.762
			(31.079)	(32.417)	(34.373)	(36.859)
He + *ortho*-H_2 $O(\nu_2=0)$						
$\Sigma(1_{01})^e$	RR	16.027	16.283	17.076	18.492	20.519
	RB	16.019	16.277	17.071	18.488	20.516
		(16.170)	(16.421)	(17.207)	(18.613)	(20.627)
$\Pi(1_{01})^e$	RR		18.773	20.648	23.108	
	RB		18.773	20.647	23.106	
			(18.888)	(20.755)	(23.205)	
$\Pi(1_{01})^f$	RR		18.330	19.623	21.508	
	RB		18.332	19.625	21.509	
			(18.445)	(19.733)	(21.610)	

Yang *et al.*

In the same paper, Yang *et al.*[42] compared their results with experiment for the state to state H_2O-He excitation cross sections at 429 cm^{-1} from the 0_{00} and 1_{01} initial states and obtained a good agreement. Our results are then also in good agreement with these experimental data.

We also performed RB-CC calculations and compared them with our RAST-CC results in Fig. 4 . As can be

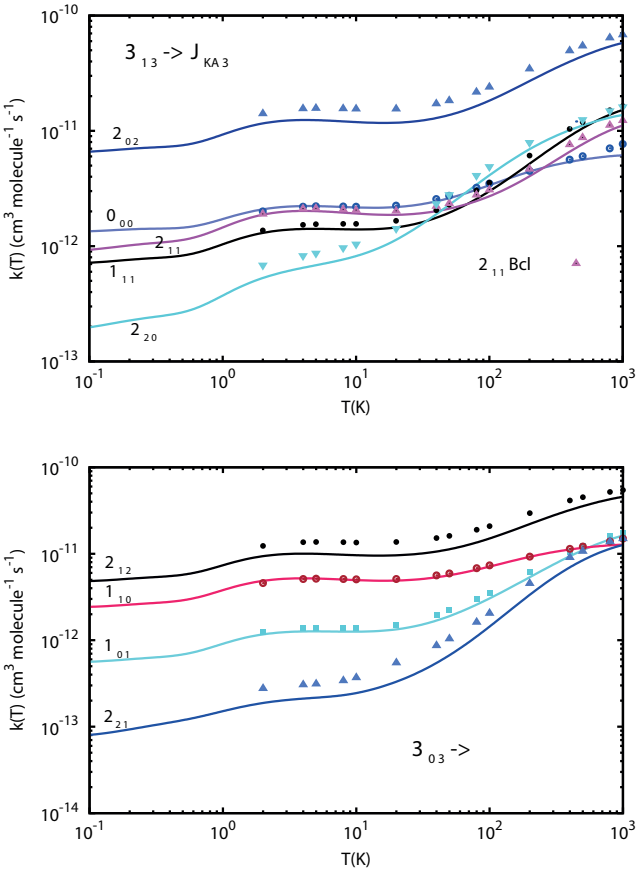

FIG. 3. RR state to state rate coefficients induced by collision with He for the two initial states 3_{03} and 3_{13} of H_2O. The final rotational state is indicated on each curve. The continuous lines are our results while the symbols are the values of Yang *et al.*[42] given in the Basecol database[41].

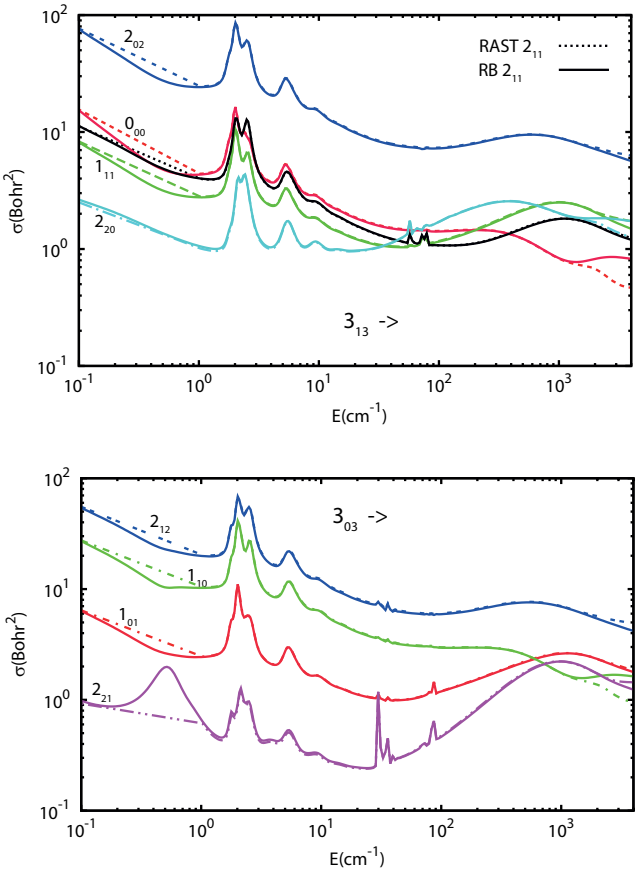

FIG. 4. Comparison between the state to state RB-CC (dashed lines) and RAST-CC (continuous lines) rotational cross sections starting from the ($\nu = 0, 3_{03}$) and ($\nu = 0, 3_{13}$) levels of H_2O colliding with He. The higher an lower panels are respectively dedicated to the *para* and *ortho* transitions.

seen in this figure the agreement between the two kinds of calculations is excellent above 1 cm^{-1}. Below this energy the resonances which can be seen on the RAST-CC curves seem to disappear at the RB-CC level as a result of the averaging over the H_2O bending angle. We conclude that rotational transitions inside the same bending level are safely described by using the rigid rotor approximation.

2. Rotational transitions inside two different bending level

Very often, for experimental detection reasons, rotational transitions are measured inside a given excited vibrational level and are assumed to be the same inside the fundamental vibrational level of the system. This is usually a good approximation for collisions involving linear molecules in different stretching states as shown recently for the collisions of CO with H_2. For this system, the resonances appearing in the state to state rotational cross sections inside two different stretching levels were found to be only slightly shifted in collision energy.

In the case of rotational states belonging to two different bending levels of a bent triatomic molecule like H_2O the situation is completely different . As a matter of fact, because of the coupling between rotation and bending, the energy classification of the states is not the same inside different bending levels. For example the 2_{20} para level is below 3_{13} inside ν_2=0 while it is the contrary inside ν_2=1. For *ortho* levels it is for example the same for 2_{21} and 3_{03}.

Furthermore, highly excited rotational levels of the fundamental bending state intersperse between rotational levels of the first excited bending level. This is for example the case of the (ν_2=0, 9_{64}) *para* level which intersperses between the (ν_2=1, 0_{00}) and (ν_2=1,1_{11}) levels. For *ortho* levels it is also the case of the (ν_2=0, 9_{63}) level for example which intersperses between the (ν_2=1,

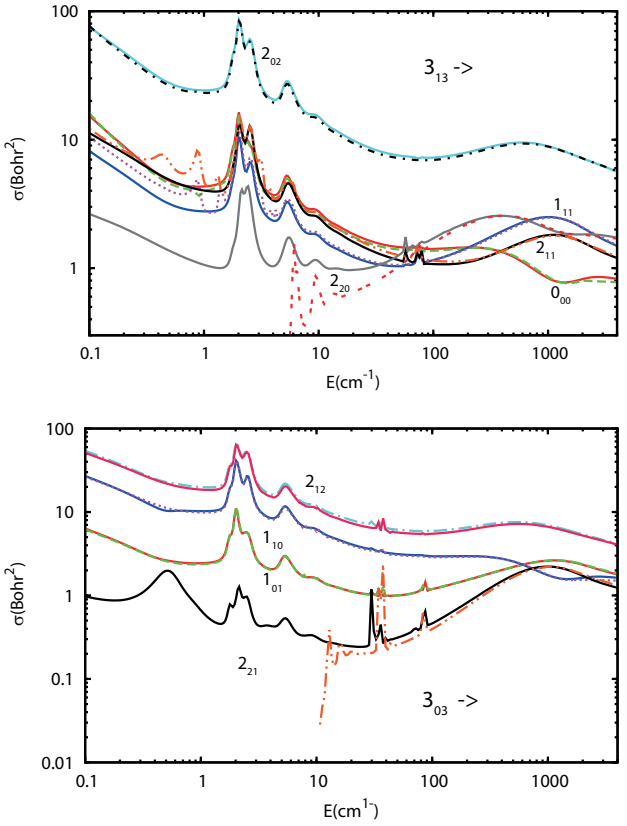

FIG. 5. Comparison between the state to state RB-CC rotational cross sections starting from the 3_{03} and 3_{13} levels of H_2O colliding with He inside the $\nu_2 = 0$ (continuous lines) and $\nu_2 = 1$ (dashed lines) levels. The higher an lower panels are respectively dedicated to the *para* and *ortho* transitions.

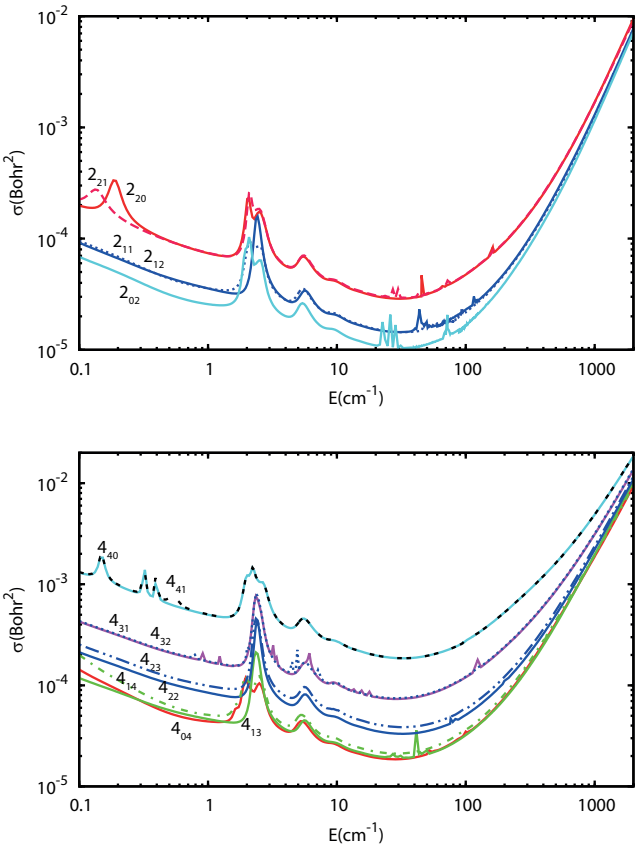

FIG. 6. RB-CC vibrational quenching cross sections of the j=4 (lower panel) and j=2(upper panel) rotational states belonging to the first excited bending level ν_2 =1 of H_2O induced by collision with He. The initial state rotational state is indicated by the values of $j_{K_a K_c}$.

1_{01}) and (ν_2=1,1_{10}) levels.

Fig. 5 shows the comparison between state to state RB-CC rotational cross sections starting from the 3_{03} and 3_{13} levels of H_2O colliding with He inside the $\nu_2 = 0$ and $\nu_2 = 1$. As can be seen in this figure most of the transitions are represented by very similar curves inside the two different bending levels. The shapes of some of the resonances are only seen to differ slightly. Conversely this figure also shows two examples of rotational transitions cross sections inside ν_2=1 differing from their counterparts inside ν_2=0. This is the case of the $3_{03} \rightarrow 2_{21}$ and $3_{03} \rightarrow 2_{20}$ transitions for the reasons mentioned above. This means that some rotational transitions inside ν_2=0 cannot be deduced from experimental measurements inside ν_2=1.

3. Rotational transitions between two different bending level

A first interesting feature of vibrational quenching is illustrated in Fig. 6 where RB-CC cross sections for each of the j=4 and j=2 multiplets belonging to the first excited bending level ν_2 =1 of H_2O are presented.

We first see that inside a multiplet the vibrational quenching cross section increases monotonously as a function of the initial rotational energy suggesting that the coupling between bending and rotation is efficiently at play. More surprisingly, the *ortho* and *para* levels the closest in energy are seen to give almost the same vibrational cross sections. This suggests that at least for this system it is sufficient for each value of j to perform calculations for the symmetry leading to the largest number of states.

From Boltzmann averaging over the distribution of rotational states inside the $H_2O(\nu_2 = 1, j = 0 - 4)$ multiplets and over collision energy, one obtains the j selected quenching rate coefficients represented in Fig. 7 . The global Boltzmann averaged ν_2 = 1,) quenching rate coefficient as well as its experimental value[23] available at 2500 K is also reported. Our computed value at 2500 K is within the experimental error bar of this measurement. This good agreement suggests that the repulsive part of our 4D PES which includes bending is also well described. The upper panel of the same figure shows the ratio of the j selected vibrational quenching rate coefficients divided by that of the j=0 state as a function of temperature

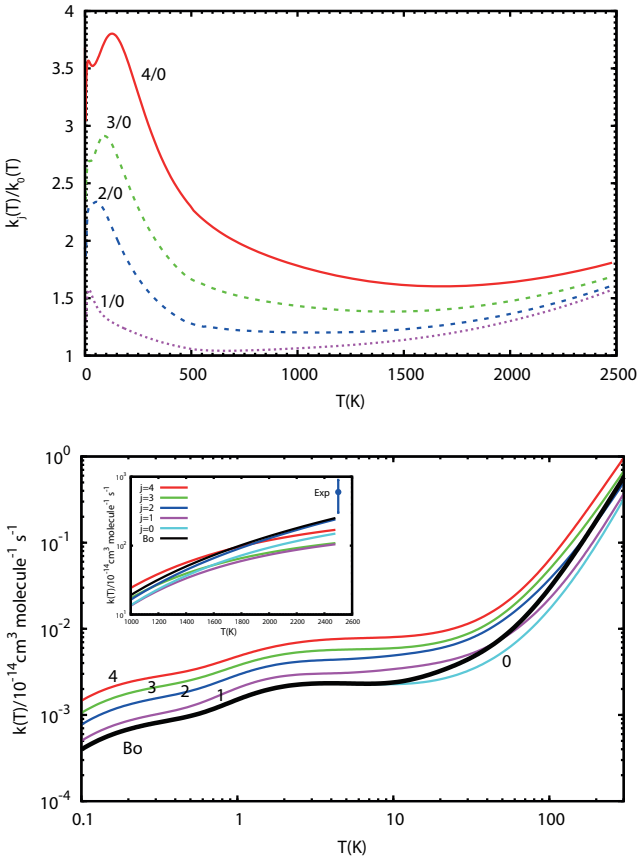

FIG. 7. Comparison with experiment[23] of the j state selected and Boltzman averaged RB-CC vibrational quenching rate coefficient of the j=0,1,2,3,4 rotational states belonging to the first excited bending level of H_2O induced by collision with He. The initial rotational state is indicated by the values of j. The higher panel shows the ratio of the j selected vibrational quenching rate coefficients divided by that of the j=0 state as a function of temperature for j=1,2,3,4.

for j=1,2,3,4. This figure demonstrates clearly that the efficiency of H_2O collisional bending relaxation increases with its rotational excitation as a result of the coupling between bending and rotation. It also shows that the coupling efficiency is low at low and high temperatures while reaching a maximum at about 15,60,100 and 120 K respectively for j=1,2,3 and 4. The lowest temperatures involve collision energies comparable to the well depth and suggest that the coupling results from this part of the intermolecular potential. For higher values of j the mechanism is more complicated as it involves also the repulsive part of the PES.

IV. SUMMARY

A Close Coupling study of the Bending relaxation of H_2O by collision with He was presented. To this aim, a new 4 D PES including the bending of H_2O was developed and tested by calculating the bound states of the He-H_2O complex. A very good agreement was obtained with the recent theoretical results of Hou *et al.*[24] demonstrating the good quality of our PES in the region of the well.
The collisional dynamics was then investigated by performing both Rigid Rotor and Rigid Bender Close Coupling calculations. As expected, the two kinds of calculations are in excellent agreement above 1 cm^{-1} for rotational transitions inside the same bending level. Below this energy the resonances appearing on the RAST-CC curves seem to disappear at the RB-CC level as a result of the averaging over the H_2O bending angle. We conclude that rotational transitions inside the same bending level are safely described by using the rigid rotor approximation. Our results were also compared with equivalent rigid rotor data available in the Basecol database. The relative average difference between our results and those of Yang *et al.* is equal to 30% as a result of both the differences between the two PES and the smaller rotational basis set used for the dynamics by Yang *et al.* Our results for the state to state H_2O-He excitation cross sections at 429 cm^{-1} from the 0_{00} and 1_{01} initial states are also in good agreement with experiment.

We then compared the same rotational transition inside two different bending levels and showed that some transitions inside the fundamental bending level cannot be deduced from their measurements inside an excited bending level. This results simply from the fact that coupling between bending and rotation changes the energy classification of the states belonging to different bending levels.

We also find that the vibrational quenching cross section increases monotonously as a function of the initial rotational energy inside a j multiplet suggesting that the coupling between bending and rotation is efficiently at play. More surprisingly, the *ortho* and *para* levels the closest in energy give almost the same vibrational cross sections. This suggest that at least for this system it is sufficient for each value of j to perform calculations for the symmetry leading to the largest number of states.

The efficiency of the H_2O collisional bending relaxation is also found to increase with its rotational excitation as a result of the coupling between bending and rotation.The coupling efficiency appears to be low at low and high temperatures while reaching a maximum between 15 and 120 K depending on the initial value of j.

SUPPLEMENTARY MATERIAL

A Fortran subroutine of the PES described in section II A is given with examples of use.

ACKNOWLEDGMENTS

We acknowledge the support from the ECOS-SUD-CONICYT project number C17E06 (Programa de Cooperación Científica ECOS-CONICYT ECOS170039). Computer time for this study was provided by the Mésocentre de Calcul Intensif Aquitain, which is the computing facility of Université de Bordeaux et Université de Pau et des Pays de l'Adour.

AVAILABILITY OF DATA

The data that support the findings of this study are available within this article and its supplementary material.

[1]E. F. van Dishoeck, E. Herbst and D. A. Neufeld, *Chem. Rev.*, 2013, **113**, 9043–9085.
[2]S. Green, *Astrophys. J. Suppl. Ser.*, 1980, **42**, 103–141.
[3]A. Palma, S. Green, D. DeFrees and A. McLean, *Astrophys. J. Suppl. Ser.*, 1988, **68**, 287–318.
[4]S. Green, S. Maluendes and A. McLean, *Astrophys. J. Suppl. Ser.*, 1993, **85**, 181–185.
[5]B. Yang, M. Nagao, W. Satomi, M. Kimura and P. Stancil, *Astrophys. J.*, 2013, **765**, 77.
[6]A. Faure, N. Crimier, C. Ceccarelli, P. Valiron, L. Wiesenfeld and M. Dubernet, *Astron. Astrophys.*, 2007, **472**, 1029–1035.
[7]M.-L. Dubernet, F. Daniel, A. Grosjean and C. Lin, *Astron. Astrophys.*, 2009, **497**, 911–925.
[8]F. Daniel, M.-L. Dubernet, F. Pacaud and A. Grosjean, *Astron. Astrophys.*, 2010, **517**, A13.
[9]F. Daniel, M.-L. Dubernet and A. Grosjean, *Astron. Astrophys.*, 2011, **536**, A76.
[10]A. Faure, P. Valiron, M. Wernli, L. Wiesenfeld, C. Rist, J. Noga and J. Tennyson, *J. Chem. Phys.*, 2005, **122**, 221102–221102.
[11]A. Faure, L. Wiesenfeld, M. Wernli and P. Valiron, *J. Chem. Phys.*, 2005, **123**, 104309.
[12]T. Stoecklin, O. Denis-Alpizar, A. Clergerie, P. Halvick, A. Faure and Y. Scribano, *J. Phys. Chem. A*, 2019, **123**, 5704–5712.
[13]O. Denis-Alpizar, T. Stoecklin, P. Halvick and M.-L. Dubernet, *J. Chem. Phys.*, 2013, **139**, 034304.
[14]T. Stoecklin, O. Denis-Alpizar, P. Halvick and M.-L. Dubernet, *J. Chem. Phys.*, 2013, **139**, 124317.
[15]O. Denis-Alpizar, T. Stoecklin and P. Halvick, *Mon. Not. Roy. Astron. Soc.*, 2015, **453**, 1317–1323.
[16]M. M. Al Mogren, O. Denis-Alpizar, D. B. Abdallah, T. Stoecklin, P. Halvick, M.-L. Senent and M. Hochlaf, *J. Chem. Phys.*, 2014, **141**, 044308.
[17]O. Denis-Alpizar, T. Stoecklin and P. Halvick, *J. Chem. Phys.*, 2014, **140**, 084316.
[18]T. Stoecklin, O. Denis-Alpizar and P. Halvick, *Mon. Not. Roy. Astron. Soc.*, 2015, **449**, 3420–3425.
[19]P. J. Dagdigian and M. H. Alexander, *J. Chem. Phys.*, 2013, **138**, 104317.
[20]J. Loreau and A. van der Avoird, *J. Chem. Phys.*, 2015, **143**, 184303.
[21]L. Ma, P. J. Dagdigian and M. H. Alexander, *The Journal of Chemical Physics*, 2012, **136**, 224306.
[22]L. Ma, P. J. Dagdigian and M. H. Alexander, *The Journal of Chemical Physics*, 2014, **141**, 214305.
[23]R. Kung and R. Center, *J. Chem. Phys.*, 1975, **62**, 2187–2194.
[24]D. Hou, Y.-T. Ma, X.-L. Zhang and H. Li, *J. Mol. Spectrosc.*, 2016, **330**, 217–227.
[25]T. H. Dunning, *J. Chem. Phys.*, 1989, **90**, 1007.
[26]S. M. Cybulski and R. Toczyłowski, *J. Chem. Phys.*, 1999, **111**, 10520.
[27]H.-J. Werner, P. J. Knowles, G. Knizia, F. R. Manby and M. Schütz, *WIREs Comput. Mol. Sci.*, 2012, **2**, 242–253.
[28]S. F. Boys and F. Bernardi, *Mol. Phys.*, 1970, **19**, 553–566.
[29]P. Valiron, M. Wernli, A. Faure, L. Wiesenfeld, C. Rist, S. Kedžuch and J. Noga, *The Journal of Chemical Physics*, 2008, **129**, 134306.
[30]T. S. Ho and H. Rabitz, *J. Phys. Chem.*, 1996, **104**, 2584.
[31]T. Stoecklin, O. Denis-Alpizar, A. Clergerie, P. Halvick, A. Faure and Y. Scribano, *J. Phys. Chem. A*, 2019, **123**, 5704–5712.
[32]S. Carter, N. Handy and B. T. Sutcliffe, *Mol. Phys.*, 1983, **49**, 745.
[33]B. T. Sutcliffe and J. Tennyson, *Molec. Phys.*, 1986, **58**, 1053–1066.
[34]J. Tennyson and B. T. Sutcliffe, *International Journal of Quantum Chemistry*, 1992, **42**, 941–952.
[35]J. Tennyson, M. A. Kostin, P. Barletta, G. J. Harris, O. L. Polyansky, J. Ramanlal and N. F. Zobov, *Computer Physics Communications*, 2004, **163**, 85 – 116.
[36]S. Green, *J. Chem. Phys.*, 1976, **64**, 3463.
[37]G. Calderoni, F. Cargnoni and M. Raimondi, *Chemical Physics Letters*, 2003, **370**, 233 – 239.
[38]K. Patkowski, T. Korona, R. Moszynski, B. Jeziorski and K. Szalewicz, *Journal of Molecular Structure: THEOCHEM*, 2002, **591**, 231 – 243.
[39]M. P. Hodges, R. J. Wheatley and A. H. Harvey, *The Journal of Chemical Physics*, 2002, **116**, 1397–1405.
[40]J. Tennyson, N. F. Zobov, R. Williamson, O. L. Polyansky and P. F. Bernath, *Journal of Physical and Chemical Reference Data*, 2001, **30**, 735–831.
[41]M. Dubernet, M. Alexander, Y. Ba, N. Balakrishnan, C. Balança, C. Ceccarelli, J. Cernicharo, F. Daniel, F. Dayou, M. Doronin *et al.*, *Astron. Astrophys.*, 2013, **553**, 50.
[42]B. Yang, M. Nagao, W. Satomi, M. Kimura and P. C. Stancil, *The Astrophysical Journal*, 2013, **765**, 77.